Communication

Anion-Selective Cholesterol Decorated Macrocyclic Transmembrane Ion Carriers

Harekrushna Behera, and Nandita Madhavan

J. Am. Chem. Soc., **Just Accepted Manuscript** • DOI: 10.1021/jacs.7b07479 • Publication Date (Web): 05 Sep 2017

Anion-Selective Cholesterol Decorated Macrocyclic Transmembrane Ion Carriers

Harekrushna Behera[ξ] and Nandita Madhavan[ξψ]*

[ξ]Department of Chemistry, Indian Institute of Technology, Madras, Tamil Nadu, India and [ψ]Indian Institute of Technology, Bombay, Maharashtra, India.

Supporting Information Placeholder

ABSTRACT Anion transporters play a vital role in cellular processes and their dysregulation leads to a range of diseases such as cystic fibrosis, Bartter's syndrome and epilepsy. Synthetic chloride transporters are known to induce apoptosis in cancer cell lines. Herein, we report triamide macrocycles that are easily synthesized and externally functionalized by pendant membrane-permeable groups. Among a variety of chains appended onto the macrocycle scaffold, cholesterol is found to be the best with an EC_{50} value of 0.44 μM. The macrocycle is highly anion-selective and transports ions *via* an OH^-/X^- antiport mechanism. The macrocycle is an interesting scaffold for ion-transport as it is able to discriminate between various anions and shows a preference for SCN^- and Cl^-. Such anion-selective transporters are highly attractive model systems to study ion-transport mechanisms and could potentially be of high therapeutic value.

Transmembrane ion-transport is mediated by carriers that ferry back and forth across the lipid bilayer or by channels that form pores in the membrane. Selective and regulated ion-transport across cell membranes is crucial for several biological processes. Particularly, the transport of anions is critical for ion homeostasis, regulating pH, maintaining osmotic balance and neural signal-transduction. [1] Several diseases such as cystic fibrosis, Bartter's syndrome, inherited kidney stone diseases, myotonia and epilepsy have been associated with dysfunction of chloride channels.[2-4] Chloride transport has also been proposed to be the key mechanism for the anticancer activity of prodigiosin and its synthetic analog obatoclax.[5-8] The ability of anion transporters to induce apoptosis in cancer cell lines has been well studied and validated.[7-13] Recently, the role of chloride transporters in reducing autophagy has also been demonstrated.[14, 15] Therefore, synthetic anion transporters are potentially attractive therapeutics and anticancer agents.

Two very basic design elements for synthesizing anion transporters are a hydrophobic domain to facilitate membrane insertion and an ion-recognition domain to enhance anion-selectivity. Attractive electrostatic forces of ammonium species[16-18] or less common non-covalent interactions such as anion-π interactions, halogen bonds, and anion-macrodipole interactions have been utilized to accelerate anion transport.[19-21] Hydrogen-bond donors such as amides,[22-25] urea,[26-30] α-Aminoxy Acids,[31] perenosins,[13] tambjamines,[32] and hydroxyl groups[33, 34] have also been widely utilized as anion-recognition domains. To gain more control over the density and location of the ion-recognition domains, macrocycles such as calixarenes,[35-37] cyclic peptides,[38, 39] calixpyrroles[40-42] and porphyrin-based organic cages[43] have been utilized as scaffolds for synthetic ion-channels/carriers. Oligoamide based macrocycles are attractive scaffolds for anion transport because the amide protons are known to be good H-bond donors for anions such as halides. Herein, we report triamide macrocycle anion transporters **1**-**4** appended with lipophilic alkyl, oligoether, cholic acid and cholesterol chains, respectively (Figure 1a). The cholesterol-containing macrocycle **4** (Figure 1b) was found to be the best ion transporter, followed by macrocycle **1**. The macrocycle **4** was anion-selective with notably higher selectivity for SCN^- and Cl^-. The mechanism of ion-transport was found to be OH^-/X^- antiport with the macrocycle behaving as a carrier.

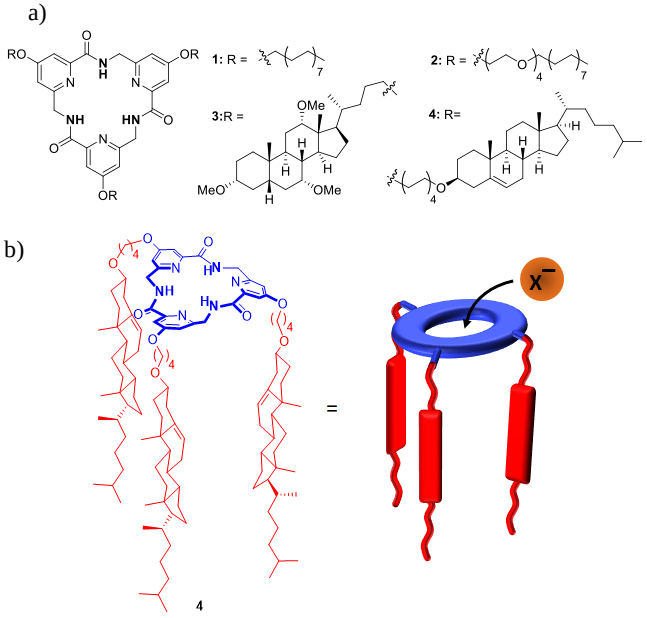

Figure 1. a) Macrocycles **1**-**4**; b) Schematic representation of the cholesterol appended macrocycle **4** – the best transporter.

Synthesis of the macrocycles was highly modular wherein desirable pendant groups could be readily appended onto the macrocycle scaffold **5** as shown in Scheme 1. Macrocycle **5** was easily accessed in one-pot using a method previously developed in our group.[44] Hydrogenolysis of the benzyl groups, followed by treatment with the appropriate R-tosyl group, afforded the requisite functionalized macrocycles **1**-**4**.

Scheme 1. General method for synthesizing macrocycles

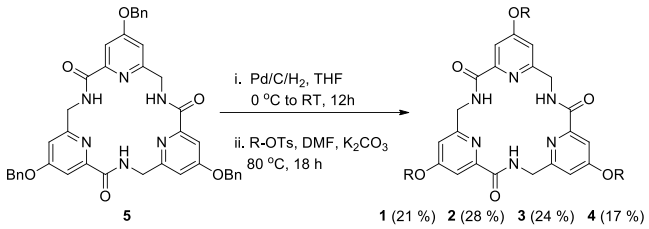

Transmembrane ion transport was assessed using vesicles made from egg yolk phosphatidyl choline (EYPC) containing pH sensitive 8-hydroxypyrene- 1,3,6-trisulfonic acid, trisodium salt (HPTS) dye as a probe (Figure 2a).[45-48] The macrocycles were allowed to equilibrate with vesicles, following which NaOH was added to increase the external pH by 0.6 units. A gradual increase in the concentration of deprotonated HPTS ($HPTS^-$) dye was observed after the base pulse (Figure 2b). This increase in internal pH of the vesicles suggested that the macrocycles were transporting ions by one of the mechanisms shown in Figure 2a. At the end of the experiment, Triton X was added to lyse the vesicles to obtain the final $HPTS^-$ concentration (to normalize the data). The rate constants for ion transport obtained by fitting the curves to a first order exponential equation showed that macrocycle **4** was the most active. The macrocycle **2** containing oligoether chains was found to show only marginally higher activity than the blank. Dose-response curves were also obtained to compare the activities of macrocycles **1**, **3** and **4**. These curves were used to obtain the EC_{50} value (effective concentration for 50 % activity) and the Hill coefficient (*n*) i.e. number of macrocycles associating with a single ion (Figure S2).[49] The EC_{50} value of macrocycle **4** was found to be very low ca. 0.44 μM, almost three times lower than those of macrocycles **1** and **3** (Figure 2c). The Hill coefficients were less than or equal to 1 indicative that the macrocycles were ion-carriers or formed monomolecular channels/stable assemblies.

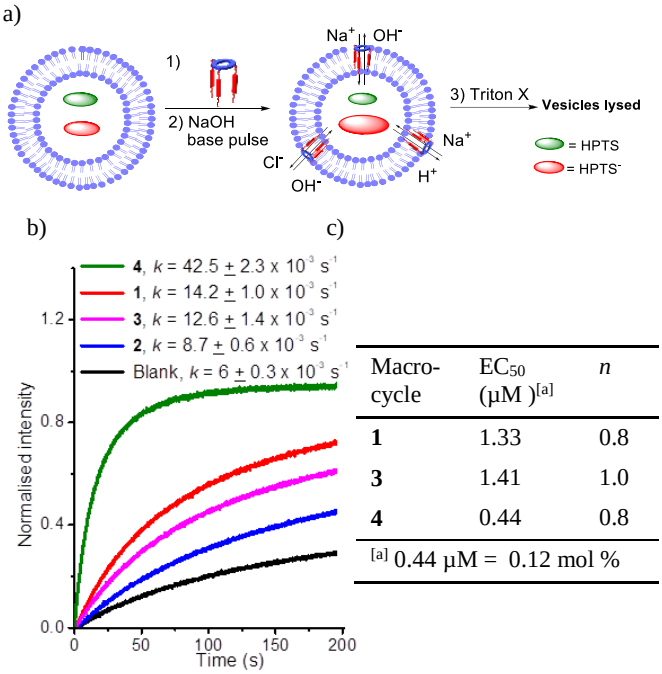

Macrocycle	EC_{50} (μM)[a]	*n*
1	1.33	0.8
3	1.41	1.0
4	0.44	0.8

[a] 0.44 μM = 0.12 mol %

Figure 2. (a) Schematic representation of the HPTS assay for ion transport, (b) Comparison of activities of macrocycles **1-4** (4.2 μM) using the HPTS assay. (c) Hill Analyses for macrocycles.

Variable temperature HPTS assays with vesicles prepared from 1,2-dipalmitoyl-sn-glycero-3-phosphocholine (DPPC) lipids were used to distinguish between the carrier and channel mechanisms. [16, 50-52] The fluid-gel transition temperature for DPPC lipid is 41 ºC. A drastic drop in ion transport activity was observed when the temperature was lowered from 45 ºC to 25 ºC (Figure 3). Such a strong dependence of activity on membrane rigidity is strongly indicative of the carrier-mechanism. To rule out expulsion of macrocycle **4** from the vesicle at lower temperatures, the vesicle suspension was subjected to size exclusion chromatography at 25 ºC prior to carrying out the high temperature HPTS assay. No significant loss in ion transport activity at 45 ºC was observed (Figure S3).

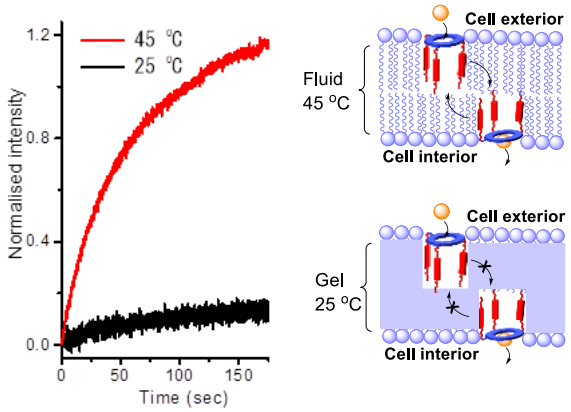

Figure. 3. Variable temperature HPTS assay with macrocycle **4** (23.1 μM) to illustrate carrier mechanism.

To check for cation-selectively, the counter cation for OH^- was varied (Li^+, Na^+, K^+, Rb^+ and Cs^+) in the base used to introduce a pH gradient in the HPTS assay. [21, 53] The ion transport rates were found to be similar irrespective of the nature of the cation (Figures 4a and 4b). Macrocycles **1-3** gave similar results (Figure S4, Table S1) suggesting that these compounds either did not transport cations or transported all cations efficiently. The *k* values in the HPTS assay carried out with NaOH were found to be independent of the extravesicular Na^+ ions concentration (Figure S5); ruling out the Na^+ /H^+ antiport or Na^+/OH^- symport mechanisms illustrated in Figure 2a.

This indicated that presumably the OH^-/ Cl^- antiport mechanism illustrated in Figure 2a was operative. To further substantiate this hypothesis, replacing Cl^- with the larger SO_4^{2-} in the extra and intravesicular solutions in the HPTS assay, showed a complete loss in activity even with large concentrations of macrocycle **4** (Figure 4c).[24] If Na^+ transport were occurring by the abovementioned mechanisms such a drop in activity would not have been observed. Furthermore, alkalization of the intravesicular solution was also observed in the absence of base pulse when vesicles were prepared in NaCl buffer and suspended in Na_2SO_4 buffer (Figure 4d).[24] Since, the SO_4^{2-} ions cannot be transported across the bilayer by the macrocycle, the changes in internal pH could only be explained by a Cl^-/OH^- antiport, driven by Cl^- efflux. Naturally, reversal of the buffer solutions resulted in acidification of the vesicular compartment due to Cl^- influx (Figure S6). To unequivocally rule out the ability of macrocycle **4** to transport sodium ions across the lipid bilayer, ^{23}Na NMR measurements were made with vesicles incubated with macrocycle **4**.[54, 55] A shift reagent ($DyCl_3$ + $Na_5P_3O_{10}$) was added to differentiate the internal and external Na^+ ions in the ^{23}Na NMR spectra (Figure 4e). Negligible line broadening was observed for the peaks indicating that no Na^+ exchange was occurring (Table S2).

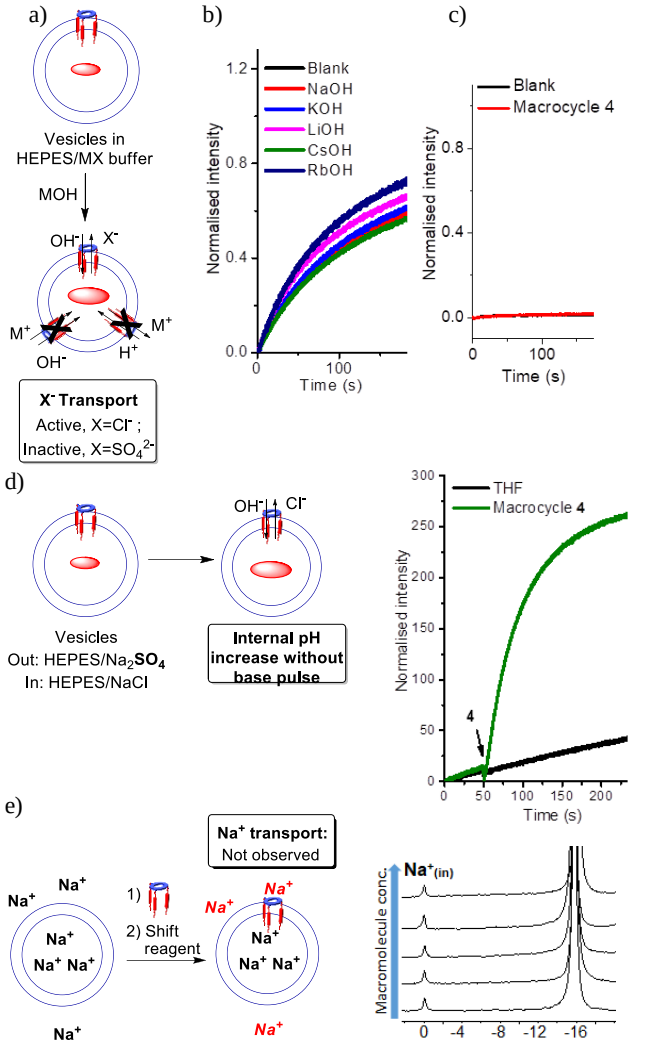

Figure 4. Assays to determine ion-selectivity. a) Schematic of HPTS assay with macrocycle **4** and normalised fluorescence vs. time plots to determine ion-transport mechanism by varying b) external cations in MOH pulse; 0.26 μM macrocycle used and c) the anion in the buffer (NaCl was replaced by Na_2SO_4); 22.2 μM macrocycle used; d) Schematic of assay and normalized fluorescence versus time plots for assay without base pulse to prove OH^-/ Cl^- antiport mechanism (2.1 μM of macrocycle used). e) Schematic of ^{23}Na NMR assay and stacked NMR plots obtained assay with different macrocycle concentrations to rule out Na^+ transport.

The selectivity studies above confirmed that the predominant ion-transport mechanism was OH^-/ Cl^- antiport. Therefore, it was not surprising that the ion transport rates were dependent on the nature of the extravesicular anions in the HPTS assay with macrocycle **4** (Figures 5a and S7). The macrocycle showed minimal transport of $NO_2^-$and CH_3COO^-. For the other anions the ion transport activity was found to be $SCN^- > Cl^- > Br^-$, ClO_4^-, I^-. The order of anion-selectivity does not directly follow the Hofmeister series. A combined effect of hydrophobicity and hydrogen bonding interactions appears to dictate the selectivity of these anions. The highest selectivity for the linear SCN^- can be explained based on the Hofmeister series. However, in the case of the other ions the order of selectivity is the reverse of the Hofmeister series. The un-functionalized macrocycle was found to bind with Cl^-.[44] A downfield shift as well as sharpening of the amide proton for macrocycle **4** was also observed upon addition of TBACl (Figure 5b). The selectivity order for the other ions is presumably dominated by the hydrogen bonding ability of the ions to the macrocyclic amides. This would explain the anti-Hofmeister selectivity i.e. $Cl^- > Br^- > I^-$ for the halides. The pyridyl groups of the macrocycle will be not be protonated in the current studies (at ~pH 7) as the pKa of pyridinium ions ranges 5.1 – 5.3 in alcohol based solvents and water.[56,57] However, the pyridyl groups in the macrocycle can be potentially exploited for pH modulated ion transport. Overall, the anion-selectivity of the macrocycles can be explained by H-bonding interactions of the anions with the amide NH bonds in the macrocycle (Figure 5c). The relative order of ion-transport activity among macrocycles **1-4** can be rationalized based on the hydrophobicity of the appended groups. The cholesterol units being the most hydrophobic improve membrane permeation and hence ion-transport activity.

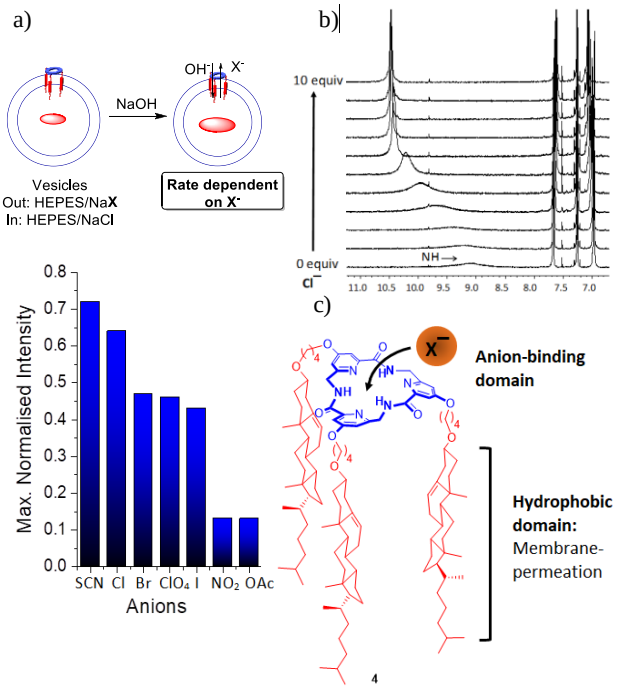

Figure. 5. a) Schematic and normalised fluorescence time courses obtained from the HPTS assay used to determine anion selectivity of macrocycle **4** (0.26 μM of macrocycle used). b) Stacked NMR plots for titration of macrocycle **4** (0.005 M) with TBACl. c) Schematic illustration for anion-selectivity and high ion transport activity of macrocycle **4**.

In summary, triamide macrocycles **1-4** appended with membrane permeable alkyl, oligoether, cholic acid and cholesterol chains, respectively, were synthesized using a modular synthetic approach. This approach allows for easy modification of the macrocycle periphery with desirable pendant groups. Macrocycle **4** containing cholesterol was the most active and had a very low EC_{50} value of 0.44 μM. The higher activity of macrocycle **4** has been attributed to the high membrane permeability of the hydrophobic cholesterol side chains. A carrier mechanism has been proposed for ion transport based on the high dependence of ion transport activity on membrane rigidity. The macrocycle was highly anion-selective and transported anions *via* an X^-/OH^- antiport mechanism. The macrocycle could discriminate among anions and showed a preference for SCN^- and Cl^-. The pyridyl units in macrocycle provide exciting opportunities for modulating the ion selectivity as well as transport activity using pH. Current efforts are focussed on regulating the ion-transport activity of the macrocycles using external stimuli such as pH and light.

ASSOCIATED CONTENT

Supporting Information

Detailed procedures, characterization of compounds, raw plots for vesicle assays, DLS data, and NMR titration data has been provided in the Supporting information. This material is available free of charge on the ACS Publications website at http://pubs.acs.org

AUTHOR INFORMATION

Corresponding Author

*E-mail: nanditam@chem.iitb.ac.in

Notes

The authors declare no competing financial interests.

ACKNOWLEDGMENT

This research was supported by DST (SR/S1/OC-41/2009), New Delhi, India. H.B. thanks IIT Madras for fellowship. We thank Dr. E. Prasad for the use of his DLS instrument.

REFERENCES

1. Hille, B. *Ion Channels of Excitable Membranes, 3rd ed*.; Sinauer Associates Inc.: Sunderland, 2001; Chapter 1.
2. Ashcroft, F. M. *Ion Channels and Disease: Channelopathies*. Academic Press: San Diego, 1999; Chapter 12.
3. Quinton, P. M. *Lancet* **2008,** *372*, 415-417.
4. Jentsch, T. J.; Hübner, C. A.; Fuhrmann, J. C. *Nat. Cell Biol.* **2004,** *6*, 1039-1047.
5. Sessler, J. L.; Eller, L. R.; Cho, W.-S.; Nicolaou, S.; Aguilar, A.; Lee, J. T.; Lynch, V. M.; Magda, D. J. *Angew. Chem. Int. Ed.* **2005,** *44*, 5989-5992.
6. Sato, T.; Konno, H.; Tanaka, Y.; Kataoka, T.; Nagai, K.; Wasserman, H. H.; Ohkuma, S. *J. Biol. Chem.* **1998,** *273*, 21455-21462.
7. Gale, P. A.; Pérez-Tomás, R.; Quesada, R. *Acc. Chem. Res.* **2013,** *46*, 2801-2813.
8. Díaz de Greñu, B.; Hernández, P. I.; Espona, M.; Quiñonero, D.; Light, M. E.; Torroba, T.; Pérez-Tomás, R.; Quesada, R. *Chem.-Eur. J.* **2011,** *17*, 14074-14083.
9. Saha, T.; Gautam, A.; Mukherjee, A.; Lahiri, M.; Talukdar, P. *J. Am. Chem. Soc.* **2016,** *138*, 16443-16451.
10. Busschaert, N.; Gale, P. A. *Angew. Chem. Int. Ed.* **2013,** *52*, 1374-1382.
11. Gale, P. A.; Davis, J. T.; Quesada, R. *Chem. Soc. Rev.* **2017,** *46*, 2497-2519.
12. Ko, S.-K.; Kim, S. K.; Share, A.; Lynch, V. M.; Park, J.; Namkung, W.; Van Rossom, W.; Busschaert, N.; Gale, P. A.; Sessler, J. L.; Shin, I. *Nat. Chem.* **2014,** *6*, 885-892.
13. Van Rossom, W.; Asby, D. J.; Tavassoli, A.; Gale, P. A. *Org. Biomol. Chem.* **2016,** *14*, 2645-2650.
14. Busschaert, N.; Park, S.-H.; Baek, K.-H.; Choi, Y. P.; Park, J.; Howe, E. N. W.; Hiscock, J. R.; Karagiannidis, L. E.; Marques, I.; Félix, V.; Namkung, W.; Sessler, J. L.; Gale, P. A.; Shin, I. *Nat. Chem.* **2017,** *9*, 667-675.
15. Rodilla, A. M.; Korrodi-Gregório, L.; Hernando, E.; Manuel-Manresa, P.; Quesada, R.; Pérez-Tomás, R.; Soto-Cerrato, V. *Biochem. Pharmacol.* **2017,** *126*, 23-33.
16. Deng, G.; Dewa, T.; Regen, S. L. *J. Am. Chem. Soc.* **1996,** *118*, 8975-8976.
17. Izzo, I.; Licen, S.; Maulucci, N.; Autore, G.; Marzocco, S.; Tecilla, P.; De Riccardis, F. *Chem. Commun.* **2008**, 2986-2988.
18. Madhavan, N.; Robert, E. C.; Gin, M. S. *Angew. Chem. Int. Ed.* **2005,** *44*, 7584-7587.
19. Jentzsch, A. V.; Hennig, A.; Mareda, J.; Matile, S. *Acc. Chem. Res.* **2013,** *46*, 2791-2800.
20. Busschaert, N.; Caltagirone, C.; Van Rossom, W.; Gale, P. A. *Chem. Rev.* **2015,** *115*, 8038-8155.
21. Gorteau, V.; Bollot, G.; Mareda, J.; Matile, S. *Org. Biomol. Chem.* **2007,** *5*, 3000-3012.
22. Cook, G. A.; Pajewski, R.; Aburi, M.; Smith, P. E.; Prakash, O.; Tomich, J. M.; Gokel, G. W. *J. Am. Chem. Soc.* **2006,** *128*, 1633-1638.
23. Busschaert, N.; Kirby, I. L.; Young, S.; Coles, S. J.; Horton, P. N.; Light, M. E.; Gale, P. A. *Angew. Chem. Int. Ed.* **2012,** *51*, 4426-4430.
24. Sidorov, V.; Kotch, F. W.; Kuebler, J. L.; Lam, Y.-F.; Davis, J. T. *J. Am. Chem. Soc.* **2003,** *125*, 2840-2841.
25. Saha, T.; Hossain, M. S.; Saha, D.; Lahiri, M.; Talukdar, P. *J. Am. Chem. Soc.* **2016,** *138*, 7558-7567.
26. McNally, B. A.; Koulov, A. V.; Lambert, T. N.; Smith, B. D.; Joos, J.-B.; Sisson, A. L.; Clare, J. P.; Sgarlata, V.; Judd, L. W.; Magro, G.; Davis, A. P. *Chem. -Eur. J.* **2008,** *14*, 9599-9606.
27. Valkenier, H.; Davis, A. P. *Acc. Chem. Res.* **2013,** *46*, 2898-2909.
28. Li, H.; Valkenier, H.; Judd, L. W.; Brotherhood, P. R.; Hussain, S.; Cooper, J. A.; Jurček, O.; Sparkes, H. A.; Sheppard, D. N.; Davis, A. P. *Nat. Chem.* **2016,** *8*, 24-32.
29. Roy, A.; Saha, D.; Mukherjee, A.; Talukdar, P. *Org. Lett.* **2016,** *18*, 5864-5867.
30. Lisbjerg, M.; Valkenier, H.; Jessen, B. M.; Al-Kerdi, H.; Davis, A. P.; Pittelkow, M. *J. Am. Chem. Soc.* **2015,** *137*, 4948-4951.
31. Li, X.; Wu, Y.-D.; Yang, D. *Acc. Chem. Res.* **2008,** *41*, 1428-1438.
32. Knight, N. J.; Hernando, E.; Haynes, C. J. E.; Busschaert, N.; Clarke, H. J.; Takimoto, K.; Garcia-Valverde, M.; Frey, J. G.; Quesada, R.; Gale, P. A. *Chem. Sci.* **2016,** *7*, 1600-1608.
33. Berezin, S. K.; Davis, J. T. *J. Am. Chem. Soc.* **2009,** *131*, 2458-2459.
34. Saha, T.; Dasari, S.; Tewari, D.; Prathap, A.; Sureshan, K. M.; Bera, A. K.; Mukherjee, A.; Talukdar, P. *J. Am. Chem. Soc.* **2014,** *136*, 14128-14135.
35. Davis, J. T.; Okunola, O.; Quesada, R. *Chem. Soc. Rev.* **2010,** *39*, 3843-3862.
36. Sidorov, V.; Kotch, F. W.; Abdrakhmanova, G.; Mizani, R.; Fettinger, J. C.; Davis, J. T. *J. Am. Chem. Soc.* **2002,** *124*, 2267-2278.
37. Jentzsch, A. V.; Emery, D.; Mareda, J.; Metrangolo, P.; Resnati, G.; Matile, S. *Angew. Chem. Int. Ed.* **2011,** *50*, 11675-11678.
38. Suga, T.; Osada, S.; Kodama, H. *Bioorg. Med. Chem.* **2012,** *20*, 42-46.
39. Rodríguez-Vázquez, N.; Amorin, M.; Alfonso, I.; Granja, J. R. *Angew. Chem. Int. Ed.* **2016,** *55*, 4504-4508.
40. Gale, P. A. *Acc. Chem. Res.* **2011,** *44*, 216-226.
41. Kim, D. S.; Sessler, J. L. *Chem. Soc. Rev.* **2015,** *44*, 532-546.
42. Tong, C. C.; Quesada, R.; Sessler, J. L.; Gale, P. A. *Chem. Commun.* **2008**, 6321-6323.
43. Benke, B. P.; Aich, P.; Kim, Y.; Kim, K. L.; Rohman, M. R.; Hong, S.; Hwang, I.-C.; Lee, E. H.; Roh, J. H.; Kim, K. *J. Am. Chem. Soc.* **2017,** *139*, 7432-7435.
44. Behera, H.; Ramkumar, V.; Madhavan, N. *Org. Bimol. Chem.* **2017,** *15*, 4937-4940.
45. Kano, K.; Fendler, J. H. *Biochim. Biophys. Acta.* **1978,** *509*, 289-299.
46. Clement, N. R.; Gould, J. M. *Biochemistry* **1981,** *20*, 1534-1538.
47. Behera, H.; Ramkumar, V.; Madhavan, N. *Chem. -Eur. J.* **2015,** *21*, 10179-10184.
48. Benke, B. P.; Madhavan, N. *Bioorg. Med. Chem.* **2015,** *23*, 1413-1420.
49. Bhosale, S.; Matile, S. *Chirality* **2006,** *18*, 849-856.
50. Otto, S.; Osifchin, M.; Regen, S. L. *J. Am. Chem. Soc.* **1999,** *121*, 10440-10441.
51. Pregel, M. J.; Jullien, L.; Canceill, J.; Lacombe, L.; Lehn, J.-M. *J. Chem. Soc, Perkin Trans.* **1995**, 417-426.
52. Cooper, J. A.; Street, S. T. G.; Davis, A. P. *Angew. Chem. Int. Ed.* **2014,** *53*, 5609-5613.
53. Sakai, N.; Matile, S. *J. Phys. Org. Chem.* **2006,** *19*, 452-460.
54. Riddell, F. G.; Hayer, M. K. *Biochim. Biophys. Acta.* **1985,** *817*, 313-317.
55. Milano, D.; Benedetti, B.; Boccalon, M.; Brugnara, A.; Iengo, E.; Tecilla, P. *Chem. Commun.* **2014,** *50*, 9157-9160.
56. Chmurzyński, L. *J. Heterocycl. Chem.* **2000**, *37*, 71-74.
57. Yan, Y.; Zhao, W.; Bhagavathy, G. V.; Faurie, A.; Mosey, N. J.; Petitjean, A. *Chem. Commun.* **2012**, *48*, 7829-7831.

Table of Contents artwork

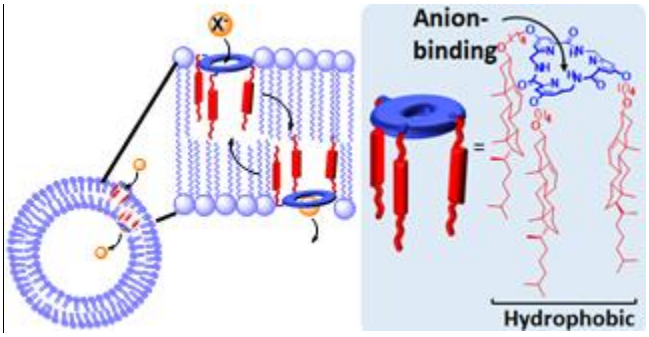

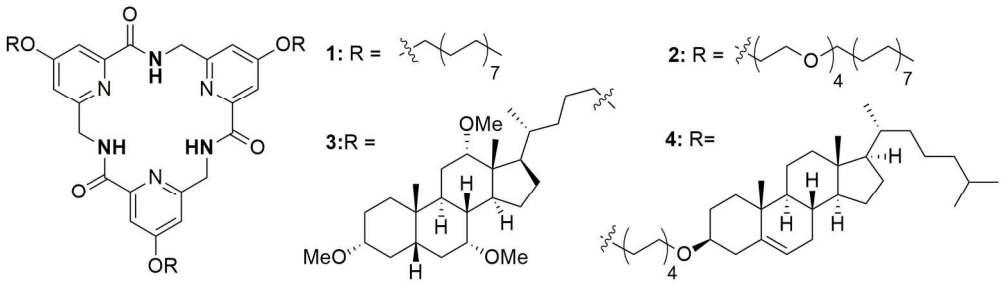

Figure 1a: Macrocycles 1-4

172x49mm (300 x 300 DPI)

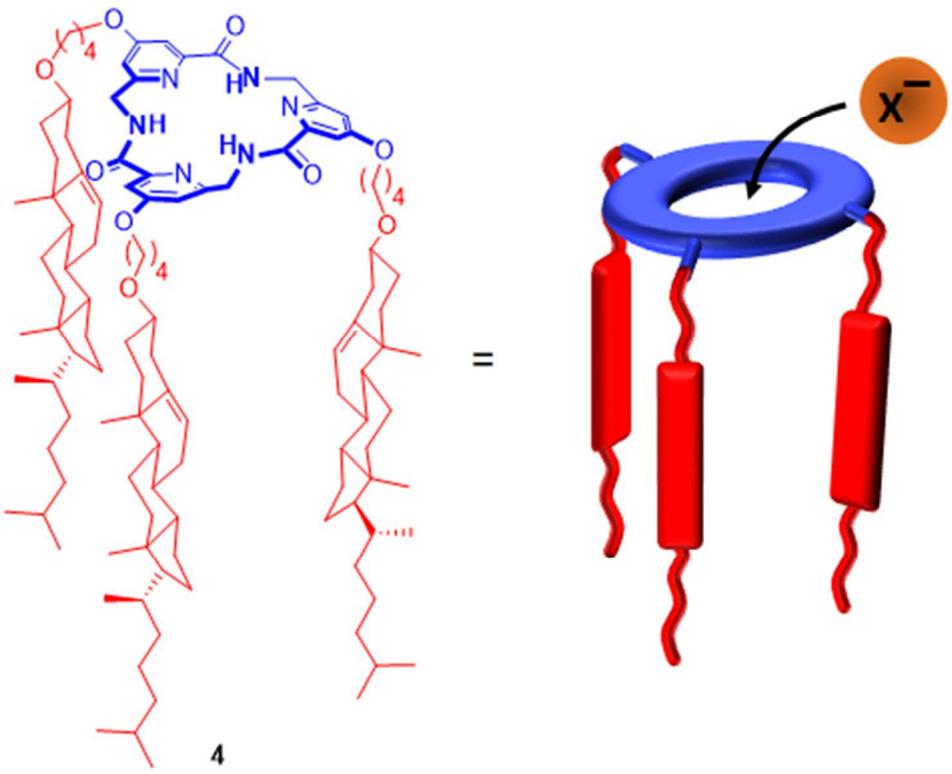

Figure 1b: Schematic representation of the cholesterol appended macrocycle 4 – the best transporter

126x101mm (96 x 96 DPI)

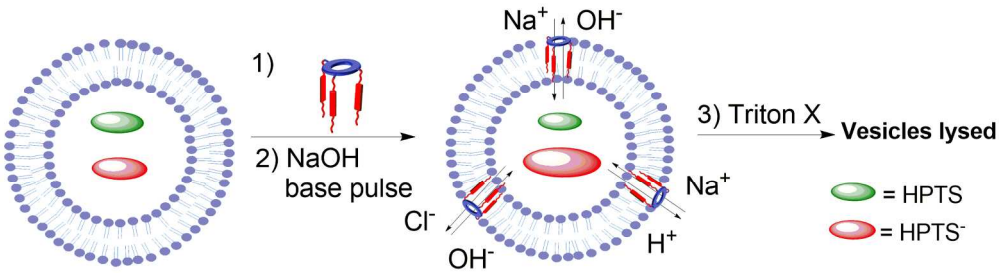

Figure 2a: Schematic representation of the HPTS assay for ion transport

185x50mm (300 x 300 DPI)

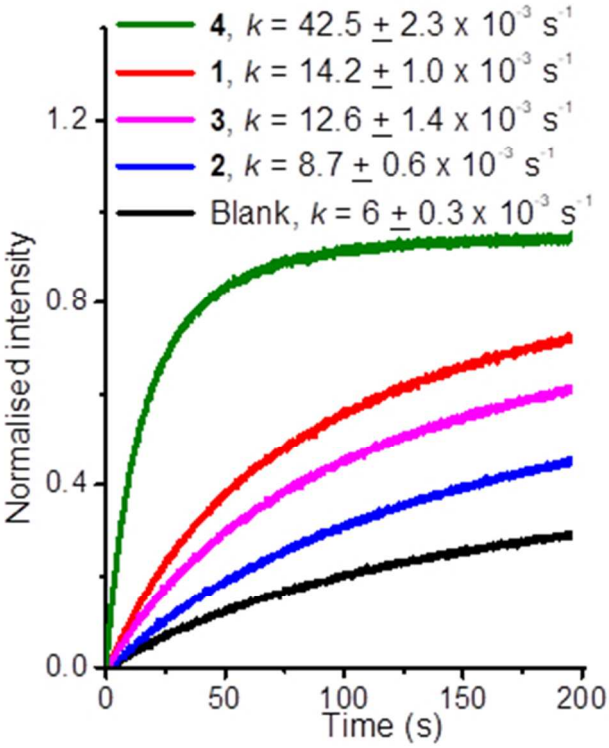

b) Comparison of activities of macrocycles 1-4 (4.2 μM) using the HPTS assay

82x98mm (96 x 96 DPI)

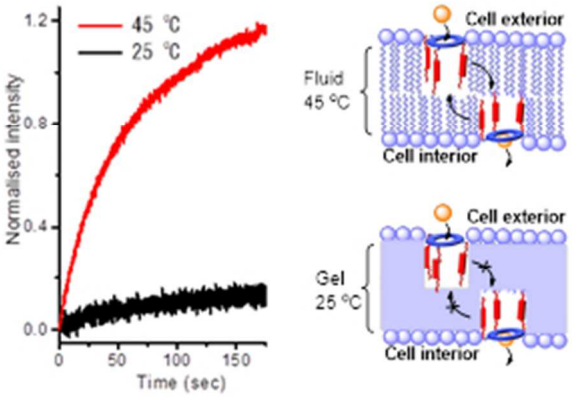

Figure 3: Variable temperature HPTS assay with macrocycle 4 (23.1 μM) to illustrate carrier mechanism.

83x56mm (96 x 96 DPI)

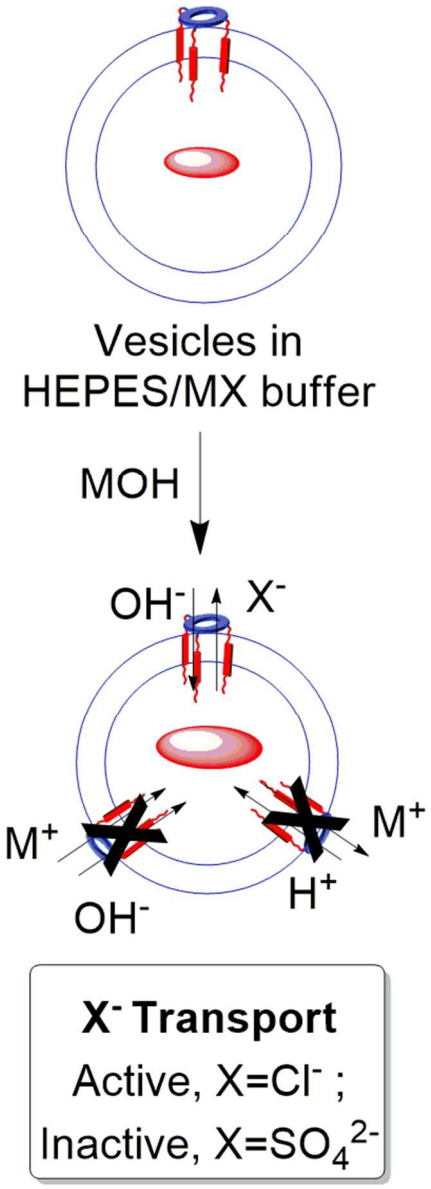

Assays to determine ion-selectivity. a) Schematic of HPTS assay with macrocycle 4 and normalised fluorescence vs. time plots to determine ion-transport mechanism by varying

35x96mm (300 x 300 DPI)

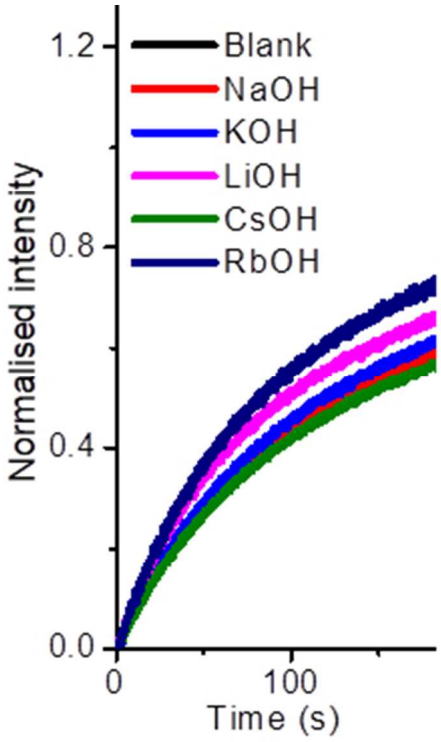

Figure 4b: Normalised fluorescence vs. time plots to determine ion-transport mechanism by varying external cations in MOH pulse; 0.26 μM macrocycle used

58x98mm (96 x 96 DPI)

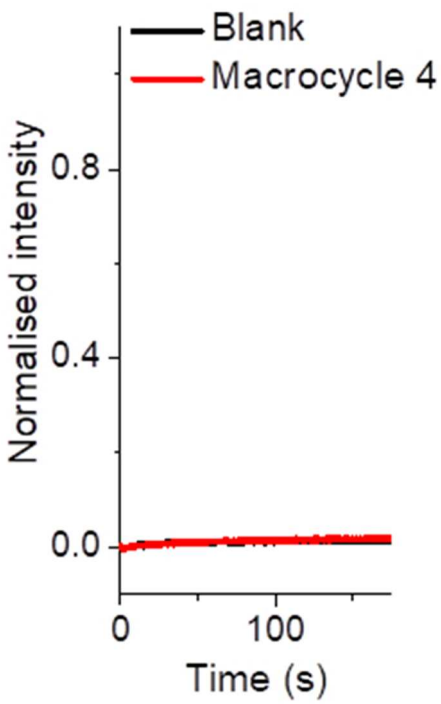

Figure 4c: Normalised fluorescence vs. time plots to determine ion-transport mechanism by varying the anion in the buffer (NaCl was replaced by Na2SO4); 22.2 μM macrocycle used;

59x93mm (96 x 96 DPI)

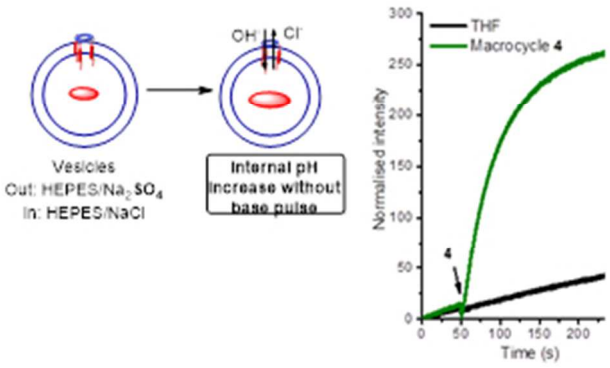

Figure 4d: Schematic of assay and normalized fluorescence versus time plots for assay without base pulse to prove OH^- / Cl^- antiport mechanism (2.1 μM of macrocycle used)

83x56mm (96 x 96 DPI)

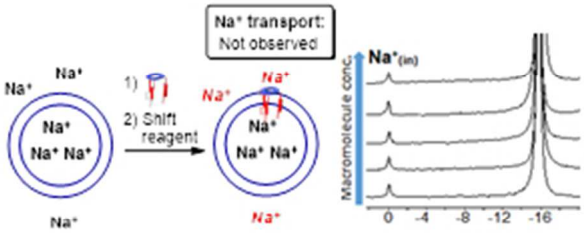

Figure 4e: Schematic of 23Na NMR assay and stacked NMR plots obtained assay with different macrocycle concentrations to rule out Na+ transport.

83x56mm (96 x 96 DPI)

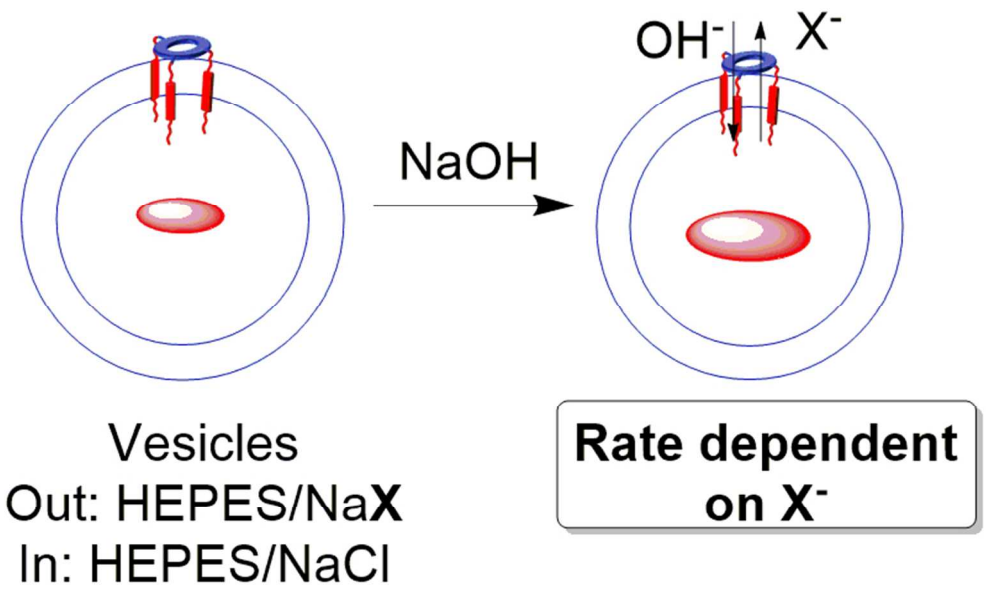

a) Schematic and normalised fluorescence time courses obtained from the HPTS assay used to determine anion selectivity of macro-cycle 4 (0.26 μM of macrocycle used).

68x41mm (300 x 300 DPI)

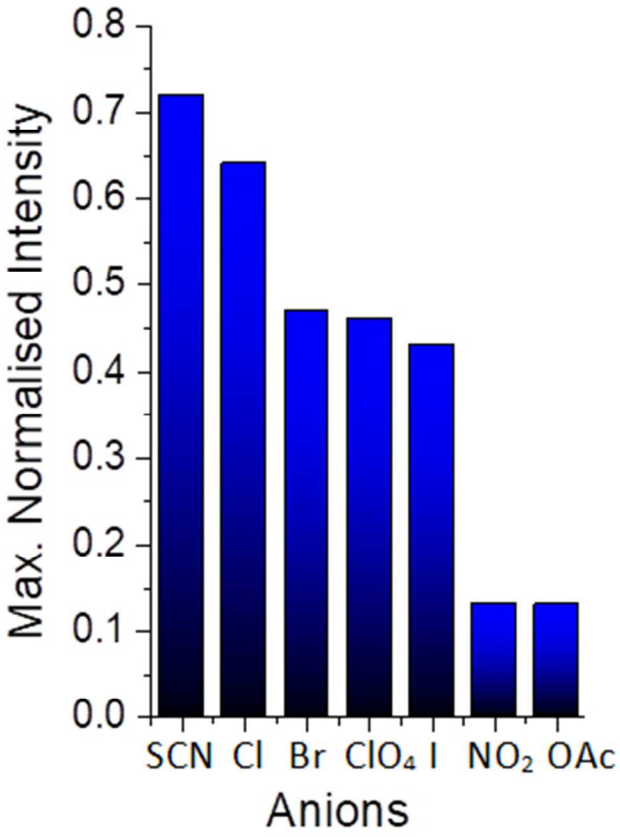

a) Schematic and normalised fluorescence time courses obtained from the HPTS assay used to determine anion selectivity of macro-cycle 4 (0.26 μM of macrocycle used).

84x112mm (96 x 96 DPI)

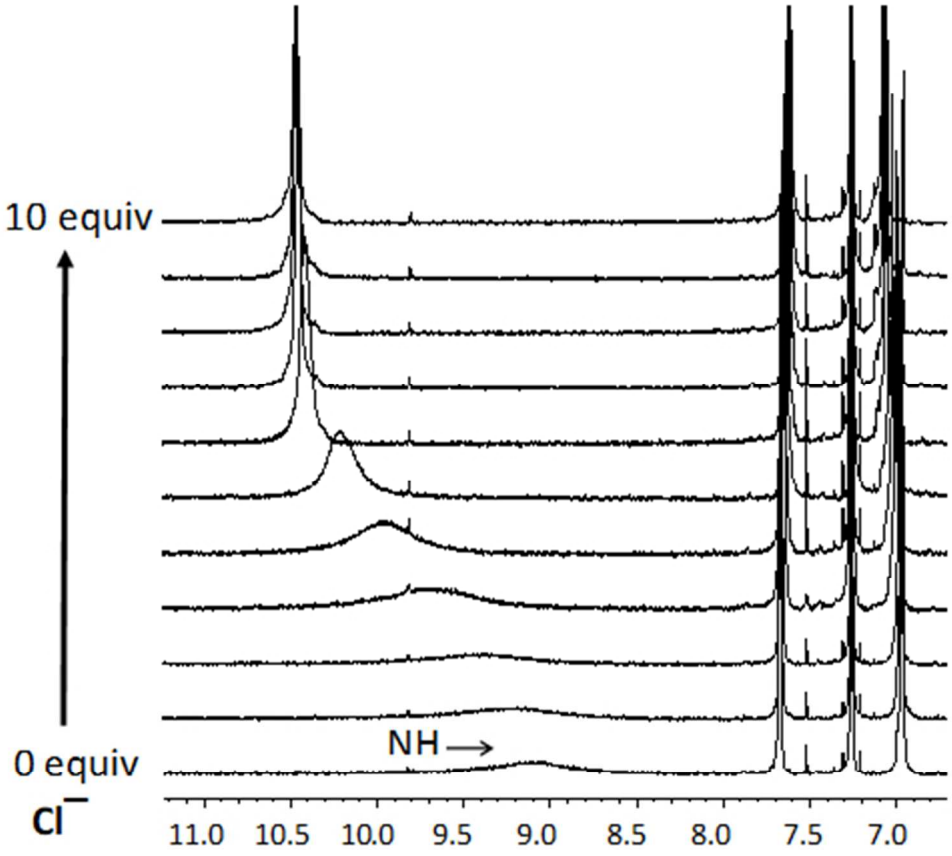

b) Stacked NMR plots for titration of macrocycle 4 (0.005 M) with TBACl.

130x115mm (96 x 96 DPI)

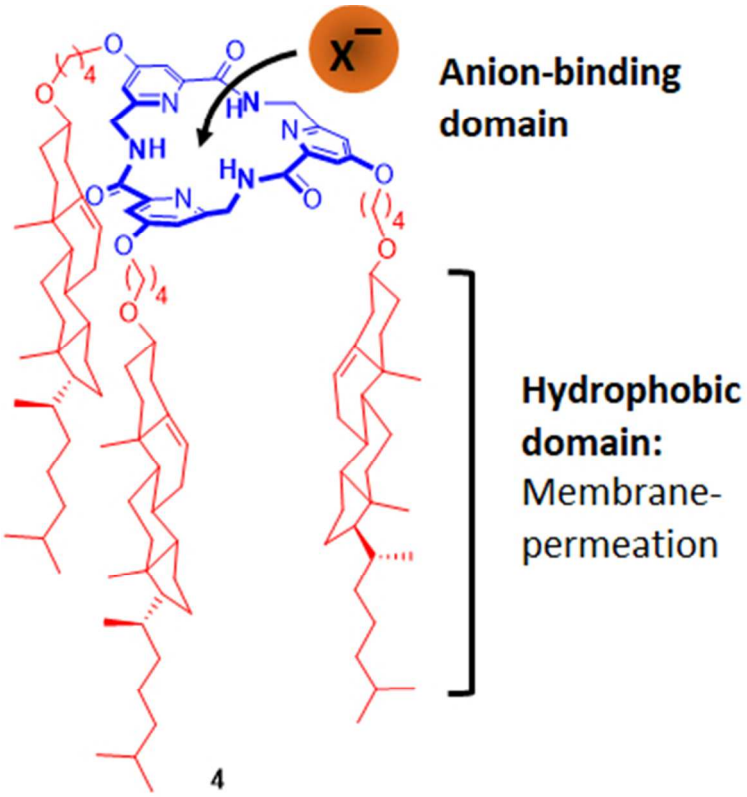

c) Schematic illustration for anion-selectivity and high ion transport activity of macrocycle 4.

108x105mm (96 x 96 DPI)

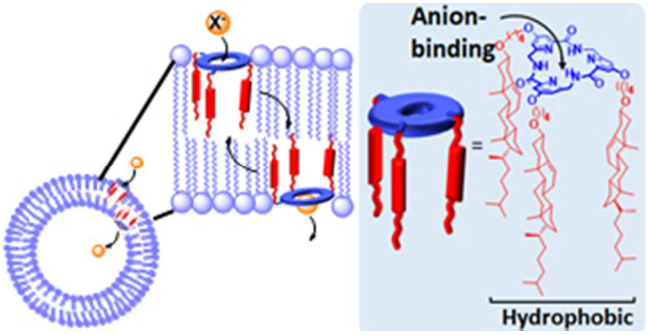

84x43mm (96 x 96 DPI)